

# ADAPTIVE SEGMENTATION OF INTERNAL BRAIN STRUCTURES IN PATHOLOGICAL MR IMAGES DEPENDING ON TUMOR TYPES

Hassan Khotanlou<sup>(1)</sup>, Jamal Atif<sup>(1)</sup>, Elsa Angelini<sup>(1)</sup>, Hugues Duffau<sup>(2)</sup>, Isabelle Bloch<sup>(1)</sup>

(1) Ecole Nationale Supérieure des Télécommunications (GET - Télécom Paris)  
CNRS UMR 5141 LTCI, Paris, France. Isabelle.Bloch@enst.fr

(2) Department of Neurosurgery, Hôpital Gui de Chauliac, CHU de Montpellier, France.

## ABSTRACT

This paper introduces a novel methodology for the segmentation of internal brain structures in MRI volumes in the presence of a tumor. The proposed method relies on an initial segmentation of the tumor. Based on the tumor's type, a set of spatial relations between internal structures, remaining stable even in presence of the pathology, is established. Segmentation and recognition of surrounding anatomical structures are based on prior knowledge about their spatial arrangement. Segmentation results on tumors inducing small or large deformations are provided to illustrate the potential of the approach.

## 1. INTRODUCTION

In brain oncology, especially when dealing with brain tumors, it is desirable to have a descriptive human brain model that can integrate tumor information extracted from MRI data such as its location, its type (cf. WHO classification [1]), its shape, its anatomo-functional positioning, as well as its influence over the surrounding brain structures (through their spatial relations for example). There is a large literature reporting works on segmentation of either cerebral structures or tumors but rarely both at the same time. This paper tries to fill this gap, by addressing the problem of segmenting internal brain structures in the presence of a tumor.

Few methods for segmentation of brain structures in the presence of a tumoral pathology have been proposed, all based on atlas registration. Tumor growth and tissue deformation models are used to constrain atlas registration. For example, a biomedical model using finite element method was proposed in [2, 3] and a simpler model based on optical-flow algorithms was introduced in [4]. Recently Cuadra *et al.*[5] and Pollo *et al.*[6] proposed a model based on radial tumor growth and using seeded atlas deformation. Nowinski and Belov [7] introduced a tumor growth model based on geometric assumption and Talairach space registration. Model computation is a time consuming process and does not apply to all types of tumor.

This work has been partially funded by GET, ANR and INCA grants. J. Atif is now with Université des Antilles et de la Guyane, Guyane, France.

The computational paradigm proposed in this paper is based on previous work from our group [8] introducing a framework for the integration of spatial relations into a deformable model, to segment normal brain structures on MRI data. Spatial relations, such as directions and distances, were represented as fuzzy subsets of the image space and incorporated into a deformable model as external forces. In this paper we extend this framework to pathological cases, where the presence of a tumor may induce important alterations of the iconic and morphometric characteristics of the surrounding structures. By understanding the spatial behavior of the tumor and its incidence on the surrounding structures (induces small or large deformations for example), we discuss the preservation of some spatial relations used for the recognition and segmentation tasks.

The tumor segmentation method is summarized in Section 2, while the proposed method for segmentation of internal brain structures is detailed in Section 3, which is the core of the paper. The approach has been applied on eight MRI data sets. In Section 4, we present their quantitative evaluation on four ones.

## 2. SEGMENTATION OF BRAIN TUMORS

Since tumor segmentation is not the focus of this paper (nor the comparison with other methods), we only briefly summarize our method. We recently proposed an original tumor segmentation approach that combines symmetry analysis and a parametric deformable model [9]. It does not require user supervision, runs on standard 3D contrast-enhanced T1-weighted MRI data, and does not make any assumption on the tumor's type. This method has been successfully applied to more than 20 cases exhibiting different types of tumors and is illustrated in Figure 1 for two different types.

## 3. ADAPTIVE SEGMENTATION OF INTERNAL CEREBRAL STRUCTURES

**A deformable model constrained with spatial relations.** Our segmentation approach combines a deformable model

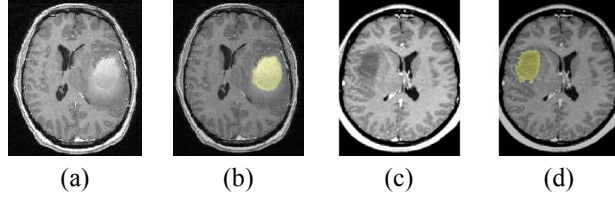


**Fig. 1.** Automated detection and segmentation of two types of tumors: (a) fully-enhanced tumor; (b) its segmentation; (c) non-enhanced tumor (low grade glioma); (d) its segmentation.

with spatial relations between brain structures [8]. These spatial relations are represented as fuzzy subsets of the image space [10]. Their integration in the evolution scheme of the deformable model relies on the introduction of a new force computed from a fuzzy set representing the fusion of spatial relations of interest.

The evolution of our deformable model is described by the following usual dynamic force equation:  $\gamma \frac{\partial \mathbf{X}}{\partial t} = \mathbf{F}_{int}(\mathbf{X}) + \mathbf{F}_{ext}(\mathbf{X})$ , where  $\mathbf{X}$  is the deformable surface,  $\mathbf{F}_{int}$  is the internal force that constrains the regularity of the surface and  $\mathbf{F}_{ext}$  is the external force. The external force combines edge and spatial relation information. It is defined as:  $\mathbf{F}_{ext} = \lambda \mathbf{F}_C + \nu \mathbf{F}_R$ , where  $\mathbf{F}_C$  is a classical data term that drives the model towards edges in the image,  $\mathbf{F}_R$  is a force derived from spatial relations and  $\lambda$  and  $\nu$  are weighting coefficients. The role of  $\mathbf{F}_R$  is to force the deformable model to stay within regions where specific spatial relations are fulfilled.

Several types of spatial relations are necessary to fully assess the structure of a given scene. We consider two main classes of spatial relations: *topological relations*, which include part-whole relations such as inclusion or exclusion, and adjacency; and *metric relations* such as distances and orientations. More complex relations can also be useful, such as “between”, “around” or “along”. Fuzzy representations are appropriate to cope with imprecision in images, in knowledge description, and to define vague relations. Our previous work in this domain was mainly based on fuzzy mathematical morphology, which allowed us to represent, in a unified framework, various spatial relations [10].

In [8], several methods to compute  $\mathbf{F}_R$  from a fuzzy set  $\mu_R$  were proposed. For instance, if  $\mu_R(x)$  denotes the degree of satisfaction of the fuzzy relation at point  $x$  (with  $\mu_R(x) \in [0, 1]$ ), and  $supp(R)$  the support of  $\mu_R$  (i.e. the set of points with non-zero membership values), then we can derive the following potential:  $P_R(x) = 1 - \mu_R(x) + d_{supp(R)}(x)$ , where  $d_{supp(R)}$  is the distance to the support of  $\mu_R$ , used to have non-zero force values outside the support. The force  $\mathbf{F}_R$  associated with the potential  $P_R$  is derived as follows:  $\mathbf{F}_R(x) = -(1 - \mu_R(x)) \frac{\nabla P_R(x)}{\|\nabla P_R(x)\|}$ . Figure 2 shows an example of a spatial relation and its corresponding force.

The adaptation of this framework to pathological cases requires addressing the fundamental question: given a pathology, what kinds of spatial relations do remain consistent, with

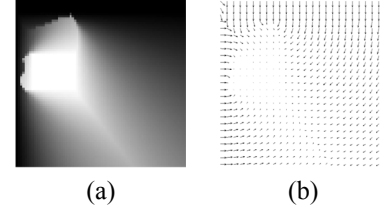


**Fig. 2.** (a) Fuzzy subset  $\mu_R$  representing the spatial relation “outside the third ventricle and below the right lateral ventricle” (highest grey level values correspond to regions where the spatial relation is best satisfied). (b) Force  $\mathbf{F}_R$  computed from  $\mu_R$ .

respect to the set of relevant relations defined for normal cases in [8]? The answer depends on the type of tumor.

**Tumor classification.** The two main brain tumor classifications used in clinical neurology are based on radiometric appearances [11] or degrees of malignancy (cf. WHO criteria [1]). The first one, also known as the Sainte-Anne classification, is partly based on the contrast enhancement of tumors, while the WHO classification is exclusively based on histological criteria. As an alternative, we consider in this work a classification of brain tumors according to their spatial characteristics and the nature of the potential alterations of the brain structural organization they induce (location, infiltration, destruction, edema...). We distinguish two main types:

- **Small deforming tumors (SD).** In this category we include tumors that are principally infiltrating without necrosis and small necrotic tumors. The whole structural brain arrangement is not significantly altered (Figures 1 (c) and 4 (a)). A further distinction is made, into subcortical (SD-SC) or peripheral (SD-P) tumors, according to their distance to the inter-hemispheric plane and depending on whether they involve deep grey nuclei or not.

- **Large deforming tumors (LD).** Tumors and lesions in this category significantly alter the surrounding brain structure arrangement. These tumors are necrotic and can be surrounded by edema (Figure 3 (a)).

Identifying the type of tumor is based on its segmentation on T1-weighted data.

**Tumor-specific spatial relations.** Some spatial relations are more stable than others in the presence of a tumor. Intuitively, topological relations imply less instability than metric ones. For example, an adjacency relation can be preserved even if large deformations are considered in a given structural organization; on the contrary metric relations, even if formulated with fuzzy sets, are prone to significant modifications in the case of large tumors and should therefore be avoided or manipulated with great care, by introducing more flexibility in their definition.

Reasoning about distances requires to take into account the granularity level of the relation expression. For example the distance predicates “far from” and “near” are naturally more vague than the predicate “at a distance of about 1cm”,

which makes them more stable. In the case of tumor-specific spatial relations, if the tumor is large deforming, only relations such as “far from” and “near” are retained. The choice of cancelling or maintaining a spatial relation in the presence of a tumor is first motivated by clinical considerations, namely the location, size and type of the tumor. Moreover, in [12], we designed a computational framework for learning spatial relations stability, from a database constituted of healthy and pathological MRI, where the main anatomical structures were manually segmented. The degree of stability was inferred from the comparison between learned spatial relations for pathological cases and for healthy ones.

Table 1 summarizes our current list of tumor-based spatial relations while Figures 3 and 4 show spatial relations involved in the segmentation of the caudate nuclei in cases of LD and SD tumors. In these examples, tumors and ventricles are first segmented. Based on the tumor’s type, specific relations to the ventricles are modeled and guide the recognition of the caudate nuclei.

Spatial characteristics of tumors		Spatial relations preserved
Large deforming (LD)		Adjacency, Direction, Distance (far, near)
Small deforming (SD)	Peripheral (SD-P)	Adjacency, Direction, Symmetry, Distance
	Subcortical (SD-SC)	Adjacency, Direction, Distance (far, near)

**Table 1.** Spatial relations for internal brain structures depending on the tumor’s type.

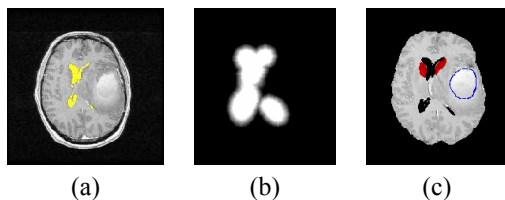


**Fig. 3.** Case of a LD tumor. (a) Segmentation of the ventricles. (b) Spatial relation “near the ventricles”, used in conjunction with directional relations for segmenting the caudate nuclei. (c) Segmented structures close to the ventricles.

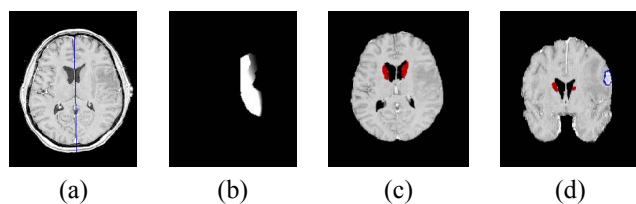


**Fig. 4.** Case of a SD-P tumor. (a) Approximate symmetry plane (useful in case of SD to process each hemisphere separately and define relations with respect to it). (b) Fusion of spatial relations “to the left of the left ventricle” and “near the left ventricle”. (c) Segmented structures on an axial slice. (d) A coronal slice.

## 4. EVALUATION

The proposed method was applied to eight clinical MRI datasets of various origins and types. We illustrate the results on four cases, for which manual segmentation of several structures was available, and which exhibit tumors with different shapes, locations, sizes, intensities and contrasts (the results on the other cases are qualitatively similar). Evaluation of the segmentation results was performed through quantitative comparisons with manual segmentations, using the error measures proposed in [13]. Let us denote by  $A$  the segmented object obtained manually and  $B$  the object segmented by the proposed method. We compute: (i) the overlap:  $\frac{|A \cap B|}{|A|}$ , (ii) the Hausdorff distance between  $A$  and  $B$  (very severe evaluation), (iii) the average distance between the surfaces of  $A$  and  $B$ . Segmentation results are illustrated in Figure 5 and quantitative evaluations are provided in Table 2, showing high accuracy. The voxel size is typically  $1 \times 1 \times 1.3 \text{ mm}^3$ , so that the average error is less than one voxel. The Hausdorff distance represents the error for the worst point, which explains its higher values. For overlap measures, values above 70% are satisfactory [14]. Although the first case exhibits strong deformations of the normal structures, the results are similar to those obtained with less deformed objects, illustrating the robustness of the adaptive approach.

Dataset	TissueType	Overlap (%)	Hausdorff (mm)	Average (mm)
1 LD	Caudate	83.35	11.5	0.85
	Ventricle	86.25	3.00	0.62
	Tumor	92.06	4.12	1.10
2 SD-SC	Caudate	82.50	3.71	0.67
	Ventricle	90.02	2.19	1.24
	Tumor	89.20	11.5	1.38
3 SD-P	Caudate	74.10	12.82	1.22
	Ventricle	88.36	11.41	0.76
	Tumor	73.52	3.47	1.22
4 SD-SC	Caudate	78.43	5.64	0.82
	Ventricle	90.32	7.57	1.82
	Tumor	81.73	2.24	1.19

**Table 2.** Segmentation evaluation for the caudate nuclei, the lateral ventricles and the tumor on four 3D MR datasets.

## 5. DISCUSSION AND CONCLUSION

The proposed segmentation framework, based on tumor-dependent preserved spatial relations, was able to incorporate some knowledge on tumoral physiology in a new and original way. For example, several teams have recently introduced biomathematical models to quantitatively describe the growth rates of gliomas visualized radiologically [15, 16]. The model in [15] takes into account the two major biological phenomena underlying the growth of gliomas at the cellular scale: proliferation and migration. Initially, this model was suggested for high-grade gliomas. Most of these anaplastic tumors have an important proliferation index, inducing a mass effect on the normal brain structures, especially in cases of large space-occupying lesions. Thus, internal cerebral structures can be

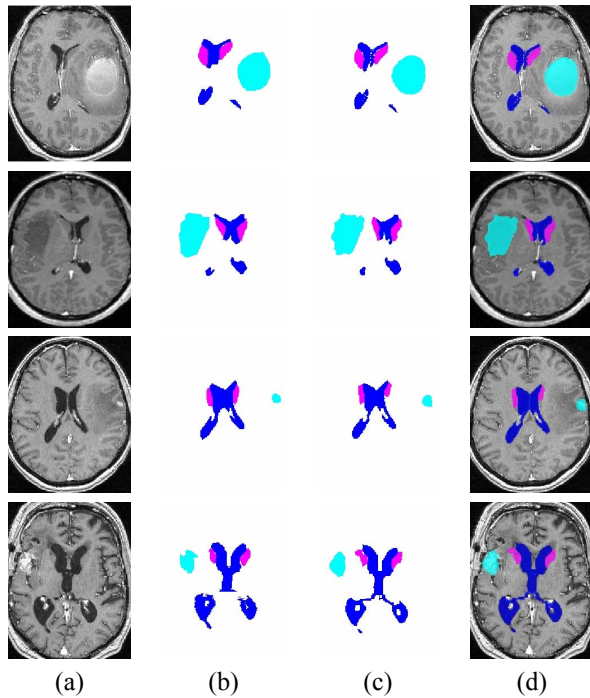


**Fig. 5.** Segmentation results. (a) Original MRI data. (b) Manual segmentation. (c) Segmentation with the proposed method. (d) Superimposition of results in (c) on MRI data (From top to bottom, tumors are LD, SD-SC, SD-P and SD-SC (cf. Table 1).

distorted, with a preservation of their spatial relations despite mechanical deformations. In the event of necrosis, very frequent in WHO grade IV gliomas (glioblastomas), it is possible that normal brain tissue is destroyed and not only distorted, eliciting neurological deficit: in these cases, topology may be modified. More recently, the same biomathematical model has also been applied to the WHO grade II gliomas, showing linear growth of mean tumor diameter [17] and anisotropic migration along white matter tract [18]. For these infiltrating tumors, there are no necrosis (i.e. no brain destruction), and the mass effect is most of the time very limited. Therefore, spatial relations of the internal cerebral structures (ventricles, deep grey nuclei and white matter bundles) are preserved, whatever the size and the location of the low-grade gliomas. Finally, it is worth noting that in addition to the natural history of the tumor, the treatment can have an impact on the segmentation of the cerebral structures and the tumor (thus their relations). This is especially true for surgery, which may induce brain deformation and changes on the functional anatomy via the resection of cerebral structures [19]. The paradigm of the proposed method should be able to handle such drastic modifications of the cerebral anatomy. Additional work, focusing on a quantitative analysis of the consistency of spatial relations over large datasets with different tumor types and behaviors is ongoing, in order to refine and complete the list of tumor-based spatial relations for each individual internal brain structure to be segmented.

## 6. REFERENCES

- [1] P. Kleihues and W. Cavenee, "(eds.) Pathology and genetics of tumours of the nervous system," USA: WHO publications Center, 2000.
- [2] S.K. Kyriacou and C. Davatzikos, "Nonlinear elastic registration of brain images with tumor pathology using a biomechanical model," *IEEE Trans. on Medical Imaging*, vol. 18, no. 7, pp. 580–592, 1999.
- [3] A. Mohamed, D. Shen, and C. Davatzikos, "Deformable registration of brain tumor images via a statistical model of tumor-induced deformation," in *MICCAI*, Oct. 2005, pp. 263–270.
- [4] M. Dawant, S.L. Hartmann, Shiyen Pan, and S. Gadamsetty, "Brain atlas deformation in the presence of small and large space-occupying tumors," *Computer Aided Surgery*, vol. 7, pp. 1–10, 2002.
- [5] M. Bach Cuadra, M. De Craene, V. Duay, B. Macq, C. Pollo, and J.-Ph. Thiran, "Dense deformation field estimation for atlas-based segmentation of pathological MR brain images," *Computer Methods and Programs in Biomedicine*, vol. 84, no. 2-3, pp. 66–75, 2006.
- [6] C. Pollo, M. Bach Cuadra, O. Cuisenaire, J. Villemure, and J. Ph. Thiran, "Segmentation of brain structures in presence of a space-occupying lesion," *Neuroimage*, vol. 24, no. 4, pp. 990–996, February 2005.
- [7] W.L. Nowinski and D. Belov, "Toward atlas-assisted automatic interpretation of MRI morphological brain scans in the presence of tumor," *Acad. Radiol.*, vol. 12, no. 8, pp. 1049–1057, 2005.
- [8] O. Colliot, O. Camara, and I. Bloch, "Integration of Fuzzy Spatial Relations in Deformable Models - Application to Brain MRI Segmentation," *Pattern Recognition*, vol. 39, pp. 1401–1414, 2006.
- [9] H. Khotanlou, O. Colliot, and I. Bloch, "Automatic Brain Tumor Segmentation using Symmetry Analysis and Deformable Models," in *ICAPR*, Kolkata, India, jan 2007, pp. 198–202.
- [10] I. Bloch, "Fuzzy Spatial Relationships for Image Processing and Interpretation: A Review," *Image and Vision Computing*, vol. 23, no. 2, pp. 89–110, 2005.
- [11] C. Dumas-Duport, "Histological grading of gliomas," *Current Opinion in Neurology and neurosurgery*, vol. 5, no. 6, pp. 924–931, 1992.
- [12] J. Atif, C. Hudelot, G. Fouquier, I. Bloch, and E. Angelini, "From Generic Knowledge to Specific Reasoning for Medical Image Interpretation using Graph-based Representations," in *IJCAI*, Hyderabad, India, jan 2007, pp. 224–229.
- [13] G. Gerig, M. Jomier, and M. Chakos, "VALMET: a new validation tool for assessing and improving 3D object segmentation," in *MICCAI*, 2001, vol. 2208, pp. 516–523.
- [14] A.P. Zijdenbos, B.M. Dawant, Richard A. Margolin, and Andrew C. Palmer, "Morphometric analysis of white matter lesions in MR images: Method and validation," *IEEE Trans. on Medical Imaging*, vol. 13, no. 4, pp. 716–724, 1994.
- [15] K.R. Swanson, C. Bridge, J.D. Murray, and E.C. Alvord, "Virtual and real brain tumors: using mathematical modeling to quantify glioma growth and invasion," *J Neurol Sci*, vol. 216, pp. 1–10, 2003.
- [16] O. Clatz, M. Sermesant, P.-Y. Bondiau, H. Delingette, S. K. Warfield, G. Malandain, and N. Ayache, "Realistic simulation of the 3D growth of brain tumors in MR images coupling diffusion with mass effect," *IEEE Trans. on Medical Imaging*, vol. 24, no. 10, pp. 1334–1346, 2005.
- [17] E. Mandonnet, J.Y. Delattre, M.L. Tanguy, K.R. Swanson, A.F. Carpentier, H. Duffau, Ph. Cornu, R. Van Effenterre, E.C. Alvord, and L. Capelle, "Continuous growth of mean tumor diameter in a subset of grade II gliomas," *Ann Neurol*, vol. 53, pp. 524–528, 2003.
- [18] S. Jbabdi, E. Mandonnet, H. Duffau, L. Capelle, K.R. Swanson, M. Pelegrini-Issac, R. Guillevin, and H. Benali, "Simulation of anisotropic growth of low-grade gliomas using diffusion tensor imaging," *Magn Reson Med*, vol. 54, pp. 616–624, 2005.
- [19] H. Duffau, "Lessons from brain mapping in surgery for low-grade glioma: insights into associations between tumour and brain plasticity," *Lancet Neurol*, vol. 4, pp. 476–486, 2005.